(Received 9 July 2024, Accepted 14 October 2024, Scheduled 17 October 2024)

A Novel Subarray Partitioning Algorithm for Small Sparse Transmitting Arrays in Microwave Power Transmission

Yuecheng Cui[1,2] and Jianxiong Li[1,2,*]

[1] School of Electronic and Information Engineering, Tiangong University, Tianjin, China
[2] Tianjin Key Laboratory of Optoelectronic Detection Technology and Systems, Tianjin, China

ABSTRACT: To enhance the performance of microwave power transmission (MPT) systems' transmitting arrays, it is essential to comprehensively consider key factors such as beam collection efficiency (BCE), the level of sidelobes outside the reception area (CSL), and expense. Current transmitting array models commonly suffer from issues like low BCE, a large number of array elements, and complex feeding systems. Addressing these issues, this paper proposes a novel transmitting array design referred to as Large Spacing Nonuniform-Excitation Sparse Planar Array (LSNSPA) and introduces a new subarray partitioning algorithm named Multi-Parameter Dynamic Weight Particle Swarm Optimization for Rectangular Subarrays (MP-DWPSO-RS). The algorithm is capable of optimizing the subarray structure, as well as the element positions and excitations, during each iteration. This paper achieves a relatively higher BCE metric than other arrays by utilizing only a small number of subarrays, through the combination of a large-spacing distribution strategy and a subarray partitioning strategy. Simulations have verified that the proposed MP-DWPSO-RS algorithm can achieve a BCE of nearly 94% when optimizing the LSNSPA with an aperture of $4.5\lambda \times 4.5\lambda$ consisting of 8×8 elements.

1. INTRODUCTION

MPT technology is widely regarded as a highly promising method for wireless energy transmission [1]. This technique enables the transmission of energy from one place to another by using microwaves, which are electromagnetic radiation with frequencies that range from 300 MHz to 300 GHz. It has a variety of applications in wireless sensor networks [2], mobile internet [3], and industrial control fields [4], as well as sensors and terminal devices such as smartphones, drones, and implantable medical devices [5]. Although the overall transmission efficiency of an MPT system is the product of the efficiencies of its various components, BCE is one of the most critical efficiencies in an MPT system. It can be defined as the ratio of the total energy emitted by the transmitting antenna to the energy that is received by the receiving antenna. Its definition is the proportion of the total power that the antenna that transmits emits to the total power that the receiving antenna receives [6]. Moreover, another crucial performance indicator in MPT is CSL, or the maximum sidelobe level observed beyond the receiving region. If every element in an array antenna is stimulated differently, it becomes necessary to build a circuit for amplifiers and a phase changer circuit for each element, which can make the entire array's feeding network extremely complex and increase the array's implementation cost. Therefore, achieving an effective simplification of the feeding network for the transmitting array in an MPT system is a current challenge in array design.

In MPT systems, subarray partitioning technology simplifies the feeding network of array antennas by grouping independent array elements into the same subarray for unified optimization [7]. This will provide the best synthesis of the sparse planar array after subarray partitioning. Creating a sensible subarray structure has significant study implications for transmitting arrays [8]. Attaining high BCE with few subarrays is the current research emphasis for small arrays.

To solve these problems, this paper suggests a Multi-Parameter Dynamic Weight Particle Swarm Optimization for Rectangular Subarrays (MP-DWPSO-RS). By using the largest generalized eigenvalue as the fitness level of the optimization process, and this method improves both the locations and excitations of array elements at the same time [9]. The innovation of this paper lies in the introduction of side length optimization factors and the use of position interval division for subarrays, achieving simultaneous optimization of element positions, element excitations, and subarray layouts, classified as a one-step optimization algorithm. This study creates a Large Spacing Nonuniform-Excitation Sparse Planar Array (LSNSPA). It has more optimization freedom than regular symmetric arrays, and the large-spacing element distribution aids in accelerating the convergence of the algorithm and effectively avoids local optima, thus further enhancing the optimization metrics. Simulation results show that the proposed algorithm is suitable for array optimization schemes with few subarrays; when the number of subarrays is 3, BCE can reach 93.21%, and CSL is -13.79 dB. This study proposes a scheme that significantly reduces costs and simplifies the design of the feeding network, making it theoretically significant for scenarios in practical applications that require only a small number of subarrays.

* Corresponding author: Jianxiong Li (lijianxiong@tiangong.edu.cn).

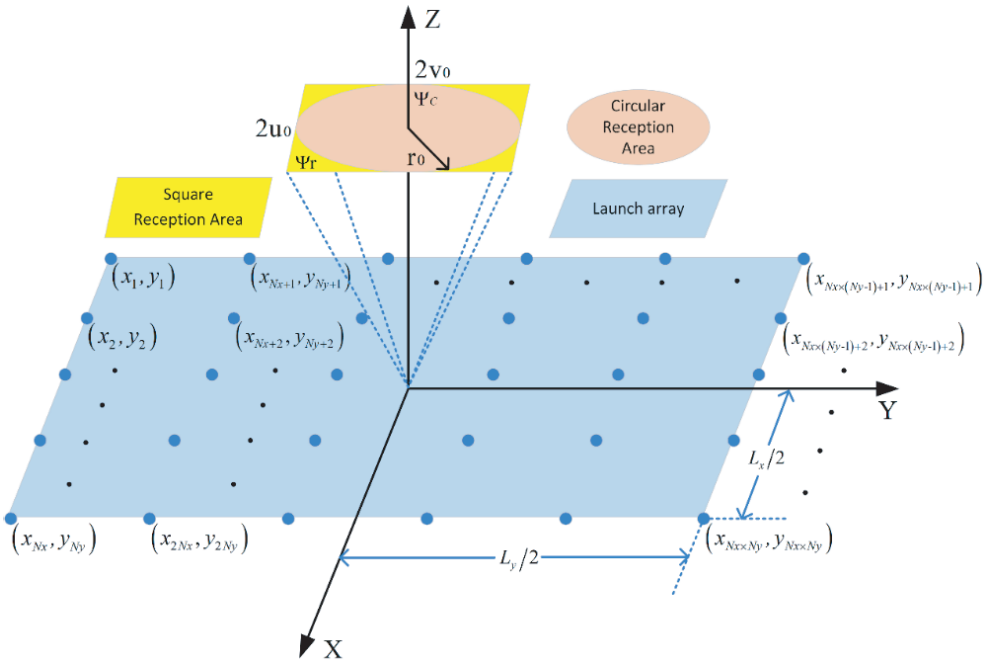

FIGURE 1. The model of the LSNSPA.

2. SPARSE PLANAR ARRAY MODEL AND SUBARRAY PARTITIONING MODEL

Figure 1 illustrates the LSNSPA model in the MPT system, and the symbols along with their meanings in the formulas mentioned in this paper are detailed in Table 1. This section will elaborate on the derivation of maximum BCE and the subarray partitioning method.

As seen in Fig. 1, let the planar array's size of the aperture be $L_x \times L_y$. On the XOY plane, M elements are dispersed at random. (x_m, y_m) is a representation of the mth element's location, and the element excitation is $\omega_m = I_m e^{-j\alpha_m}$. According to [9], substituting these parameters into a rectangular planar pattern function yields the directional pattern function of the LSNSPA:

$$F(u,v) = \sum_{m=1}^{M} \omega_m e^{ik(ux_m + vy_m)} \tag{1}$$

where k is the wave number, and $u = \sin(\theta)\cos(\varphi)$ and $v = \sin(\theta)\sin(\varphi)$ are the two angular coordinates that describe the radiation range of the array. The received power P_Ψ within the square-shaped reception space $\Psi = \{(u,v) : -u_0 \le u \le u_0, -v_0 \le v \le v_0\}$ and the total power P_Ω within the whole viewable area $\Omega = \{(u,v) : u^2 + v^2 = 1\}$ can be expressed as:

$$\begin{cases} P_\Psi = \int_\Psi |F(\theta,\varphi)|^2 \, dudv \\ P_\Omega = \int_\Omega |F(\theta,\varphi)|^2 \, dudv \end{cases} \tag{2}$$

From Eq. (2), the general notation for BCE can be written as follows:

$$BCE = \frac{P_\Psi}{P_\Omega} = \frac{\int_\Psi |F(\theta,\varphi)|^2 \, dudv}{\int_\Omega |F(\theta,\varphi)|^2 \, dudv} \tag{3}$$

Let $V_m(u,v) = e^{ik(ux_m + vy_m)}$, and we can rewrite the array pattern function as:

$$F(u,v) = \sum_{m=1}^{M} \omega_m V_m(u,v) \tag{4}$$

in this context, $\omega = [\omega_1, \omega_2, \ldots, \omega_M]$ can be represented as the element excitation vector of the array, and $V(u,v) = [e^{-ik(ux_1+vy_1)}, e^{-ik(ux_2+vy_2)}, \ldots, e^{-ik(ux_M+vy_M)}]^H$ can be represented as the element direction vector of the array. By using the aforementioned equation, we can derive the expression for the beam pattern function of the LSNSPA given the known array element direction vector $V(u,v)$ and the element excitation vector ω. Based on Eq. (4), BCE can be represented as:

$$BCE = \frac{\int_\Psi \omega^H V(u,v) V^H(u,v) \omega \, dudv}{\int_\Omega \omega^H V(u,v) V^H(u,v) \omega \, dudv} = \frac{\omega^H Z \omega}{\omega^H Q \omega} \tag{5}$$

wherein:

$$\begin{aligned} Z &= \int_\Psi V(u,v) V^H(u,v) \, dudv \\ Q &= \int_\Omega V(u,v) V^H(u,v) \, dudv \end{aligned} \tag{6}$$

Furthermore, the peak sidelobe value beyond the receiving area is specified as the CSL, which is a metric for assessing the transmitting array's performance. CSL can be written as follows [9]:

$$CSL(\text{dB}) = 10lg \frac{\max_{\theta,\varphi \notin \Psi} |F(\theta,\varphi)|^2}{\max_{\theta,\varphi \in \Omega} |F(\theta,\varphi)|^2} \tag{7}$$

TABLE 1. The list of symbols.

Symbols	Meanings
k	the wave number
m, M	the number of array elements
n, N	the number of subarrays
$d_{\min}$	the minimum element spacing
L_x, L_y	the planar array's size of the aperture
ω_m	the element excitation
I_m	the excitation amplitude
α_m	the excitation phase
x_m, y_m	the element's location
u, v	the angular coordinates that describe the radiation range of the array
BCE	the beam collection efficiency
CSL	the level of sidelobes outside the reception area
P_Ψ	the received power
P_Ω	the total power
Ψ	the square-shaped reception space
Ω	the whole viewable area
V	the element direction vector of the array
θ, φ	the pitch angle and azimuth angle of the array
ω^{opt}	the optimal element excitation vector
$\eta_{\max}$	the maximum generalized eigenvalue
B_X, B_Y	the side length vector of the subarray
SR	the subarray division matrix
I_{iv}	the initial element excitation vector
I_{sub}	the subarray excitation vector
I_{sub_all}	the element excitation vector after subarray partitioning
V_x, V_{bx}, V_{by}	the element velocity and the side length update speed
$pbest$	the local optimal individual
$pbest_x, pbest_{bx}, pbest_{by}$	the positions of the elements and the subarray side lengths corresponding to the local optimal individual
$gbest$	the global optimal individual
$gbest_x, gbest_{bx}, gbest_{by}$	the positions of the elements and the subarray side lengths corresponding to the global optimal individual

The array's receiving matrix and transmitting matrix are represented respectively. According to [9], we can transform the problem of solving the maximum BCE of the LSNSPA into solving the maximum generalized eigenvalue of the matrix equation, that is:

$$\begin{aligned} Z\omega^{opt} &= \eta_{\max} Q\omega^{opt} \\ BCE_{\max} &= \eta_{\max} \end{aligned} \tag{8}$$

Furthermore, to divide the subarrays, we compare the maximum value of the element position coordinates with the maximum random side length of the rectangular subarray. The division method is shown in Fig. 2.

The side length vector can be represented as:

$$\begin{aligned} B_X &= [bx_1, bx_2, \ldots, bx_N] \\ B_Y &= [by_1, by_2, \ldots, by_N] \end{aligned} \tag{9}$$

Based on Eq. (9), the side length optimization model has the following expression:

$$\begin{cases} \text{find} \quad B_X = [bx_1, bx_2, \ldots, bx_N]^H \\ \qquad\quad B_Y = [by_1, by_2, \ldots, by_N]^H \\ \text{maximize} \quad BCE\,(B_X, B_Y) \\ \text{subject} \quad (a)\, bx_N = L_x/2, \quad by_N = L_y/2; \\ \qquad\quad (b)\, d_{\min}/2 \le bx_n \le L_x/2, \\ \qquad\qquad d_{\min}/2 \le by_n \le L_y/2, \\ \qquad\qquad n = \{1, 2, \ldots, N\}; \\ \qquad\quad (c)\, bx_{n+1} - bx_n \ge d_{\min}, \\ \qquad\qquad by_{n+1} - by_n \ge d_{\min}, \\ \qquad\qquad n = \{1, 2, \ldots, N-1\}; \end{cases} \tag{10}$$

Subarray partitioning method: $\text{Min}\,(bx_n, by_n) \le \text{Max}(x_m, y_m) < \text{Max}\,(bx_{n+1}, by_{n+1})$; $m \in (1, M)$, $n \in (1, N-1)$, this indicates that the nth subarray contains the mth element.

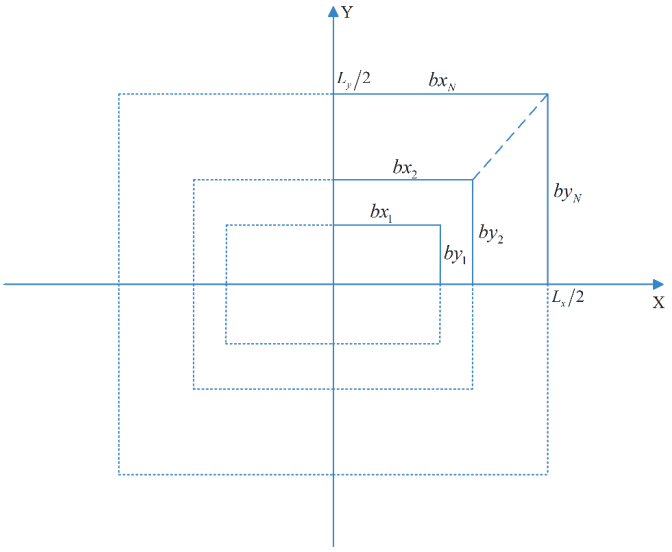

FIGURE 2. Subarray Division Model.

Let the subarray division matrix SR be an $M \times N$ matrix, which represents dividing M elements into different subarrays and can be expressed as:

$$SR = \begin{bmatrix} R_{11} & R_{12} & \dots & R_{1N} \\ R_{21} & R_{22} & \dots & R_{2N} \\ \vdots & \vdots & \ddots & \vdots \\ R_{M1} & R_{M2} & \dots & R_{MN} \end{bmatrix}$$

$$R_{mn} = \begin{cases} 1 & The\ mth\ element\ \in\ The\ nth\ subarray \\ 0 & The\ mth\ element\ \notin\ The\ nth\ subarray \end{cases}$$

$$m = 1, 2, \dots, M; \quad n = 1, 2, \dots, N. \tag{11}$$

Make sure that each element belongs to one subarray by satisfying the condition:

$$\sum_{n=1}^{N} R_{mn} = 1, \quad m = 1, 2, \dots, M \tag{12}$$

For the initial element excitation vector, provide the following definition:

$$I_{i\nu} = [I_1, I_2, \dots, I_M]^H \tag{13}$$

The subarray excitation vector is defined as follows:

$$I_{sub} = \left[I_1^{sub}, I_2^{sub}, \dots, I_N^{sub}\right]^H \tag{14}$$

The excitation formula for each subarray is calculated as follows:

$$I_n^{sub} = \frac{\sum_{m=1}^{M} R_{mn} \cdot I_m}{\sum_{m=1}^{M} R_{mn}}, \quad n = 1, 2, \dots, N \tag{15}$$

By multiplying the subarray partitioning matrix by the subarray excitation vector, the element excitation vectors after subarray partitioning can be obtained, as shown below:

$$I_{sub\_all} = SR \cdot I_{sub} \tag{16}$$

Therefore, according to Eq. (5), Eq. (15), and Eq. (16), we can deduce that:

$$BCE = \frac{(I_{sub\_all})^H \cdot Z \cdot I_{sub\_all}}{(I_{sub\_all})^H \cdot Q \cdot I_{sub\_all}} \tag{17}$$

3. MP-DWPSO-RS ALGORITHM AND ITS UTILIZATION ON THE LSNSPA

3.1. Overview of the LSNSPA Model Based on MP-DWPSO-RS

Through multiple simulations, we have found that for intelligent optimization algorithms such as particle swarm optimization, appropriately increasing the minimum element spacing can accelerate convergence. Therefore, this paper proposes a sparse rectangular planar array model with a large spacing distribution that experiences nonuniform stimulation. The optimization model of the LSNSPA using the MP-DWPSO-RS algorithm can be represented as:

$$\begin{cases} \text{find } [X] = [x_1, x_2, \dots, x_M, y_1, y_2, \dots, y_M]^H \\ \quad [B_X, B_Y] = [bx_1, bx_2, \dots, bx_N, by_1, by_2, \dots, by_N]^H \\ \text{maximize } BCE_{\max}[X, B_X, B_Y] \\ \text{subject } (a)\ -L_x/2 \le x_m \le L_x/2,\ m = \{1, 2, \dots, M\}; \\ \quad (b)\ -L_y/2 \le y_m \le L_y/2,\ m = \{1, 2, \dots, M\}; \\ \quad (c)\ \sqrt{(x_{m_1} - x_{m_2})^2 + (y_{m_1} - y_{m_2})^2} \ge d_{\min}, \\ \quad\quad m_1, m_2 \in \{1, 2, \dots, M\},\ m_1 \ne m_2; \\ \quad (d)\ (x_1, y_1) = (-L_x/2, -L_y/2), \\ \quad\quad (x_{end}, y_1) = (L_x/2, -L_y/2); \\ \quad (e)\ (x_1, y_{end}) = (-L_x/2, L_y/2), \\ \quad\quad (x_{end}, y_{end}) = (L_x/2, L_y/2); \\ \quad (f)\ d_{\min}/2 \le bx_n \le L_x/2, \\ \quad\quad d_{\min}/2 \le by_n \le L_y/2,\ n \in \{1, 2, \dots, N\}; \\ \quad (g)\ bx_{n+1} - bx_n \ge d_{\min}, \\ \quad\quad by_{n+1} - by_n \ge d_{\min},\ n \in \{1, 2, \dots, N-1\}; \\ \quad (h)\ bx_N = L_x/2,\ by_N = L_y/2; \end{cases} \tag{18}$$

The model aims to maximize BCE as the optimization objective, with the optimization variables being the element positions and side length vector. The element positions in this model are randomly distributed, offering higher degrees of optimization freedom than symmetrically distributed array models. Since small arrays have smaller apertures and fewer elements than large arrays, their overall complexity is relatively low, making the strategy of large-spacing random distribution suitable for small arrays to enhance optimization metrics.

3.2. Overview of the MP-DWPSO-RS Algorithm

MP-DWPSO-RS is an improved algorithm based on DWPSO that incorporates multi-parameter and subarray partitioning to propose a comprehensive optimization algorithm for planar

The pseudo-code of the MP-DWPSO-RS

Initialization parameters.
Initialize element position (x_m, y_m) and subarray side lengths b_{x_n}, b_{y_n}.
Initialize particle velocities V_x and side length velocities V_{bx}, V_{by}.
For $t = 1:T$
  For $NP_t = 1:NP$
    Update subarray partitioning matrix SR.
    Calculate subarray excitation I_{sub} and BCE.
    Update local optimal individual $pbest$.
    Update particle velocities V_x and side length velocities V_{bx}, V_{by}.
    Update element position (x_m, y_m) and subarray side lengths b_{x_n}, b_{y_n}.
  End
Update global optimal individual $gbest$.
End
Output the above parameters.

FIGURE 3. The pseudo-code of the MP-DWPSO-RS.

transmit arrays. Here are the specific steps of the MP-DWPSO-RS algorithm:

Step 1: Initialize parameters. Initialize the number of elements (M), the number of subarrays (N), the planar array's size of the aperture $(L_x \times L_y)$, element positions (x_m, y_m), the element velocity (V_x), receiving area (Ψ), subarray side length (B_X, B_Y), side length update speed (V_{bx}, V_{by}), current iteration number (t), and the number of iterations (T), etc.

Step 2: According to the subarray partitioning method mentioned in this paper, partition the subarrays and calculate the subarray excitations using the formula, thereby obtaining the element excitations after subarray partitioning, and calculate the BCE value in Eq. (3).

Step 3: Update the element positions (x_m, y_m) and element update speed V_x according to Eq. (19).

$$\begin{aligned} w &= w_{\max} - (w_{\max} - w_{\min}) \times (t/T)^2 \\ V_{x_{t+1}} &= w \times V_{x_t} + c_1 \times rand \times (pbest_{x_t} - x_t) \\ &\quad + c_2 \times rand \times (gbest_{x_t} - x_t) \\ x_{t+1} &= x_t + V_{x_{t+1}} \end{aligned} \tag{19}$$

Step 4: Calculate the side length update speed (V_{bx}, V_{by}) according to Eq. (20).

$$\begin{aligned} V_{bx_{t+1}} &= w \times V_{bx_t} + c_1 \times rand \times (pbest_{bx_t} - bx_t) \\ &\quad + c_2 \times rand \times (gbest_{bx_t} - bx_t) \\ bx_{t+1} &= bx_t + V_{bx_{t+1}} \\ V_{by_{t+1}} &= w \times V_{by_t} + c_1 \times rand \times (pbest_{by_t} - by_t) \\ &\quad + c_2 \times rand \times (gbest_{by_t} - by_t) \\ by_{t+1} &= by_t + V_{by_{t+1}} \end{aligned} \tag{20}$$

Step 5: Update the local optimal individual $(pbest)$ and global optimal individual $(gbest)$ according to Eq. (21).

$$\begin{aligned} &if\ pbest \le BCE \\ &pbest = BCE \\ &end \\ &gbest = \max(pbest) \end{aligned} \tag{21}$$

The above formula uses a dynamic weight calculation method that has nonlinear characteristics and represents the current iteration number. In the early stages of the algorithm, a large weight coefficient facilitates global search, allowing particles to explore the solution space more widely. Therefore, in the early iterations, the weight should be set as high as possible. In the later stages of iteration, a low weight coefficient facilitates local search, enabling particles to conduct detailed searches near known solutions. The MP-DWPSO-RS algorithm can effectively transition from global search to local search by using dynamic weights, which represent the local learning factor and global learning factor, respectively.

Step 6: Determine if t has reached the maximum number of iterations, and if not, return to step 2; otherwise output $gbest$.

By following the above steps, we can obtain the maximum BCE value after subarray partitioning. The algorithm is capable of simultaneously optimizing the element positions and excitations during each iteration, classifying it as a one-step optimization algorithm. Additionally, by combining subarray partitioning techniques with a multi-parameter particle swarm optimization algorithm, it becomes advantageous in searching for the fittest individuals within the population. Fig. 3 displays the pseudo-code for the MP-DWPSO-RS algorithm.

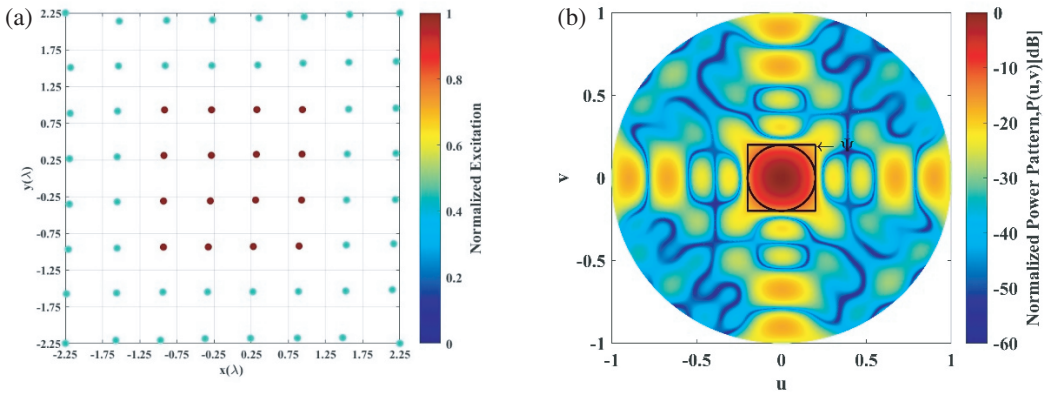

FIGURE 4. The simulation results of the LSNSPA when $N = 2$.

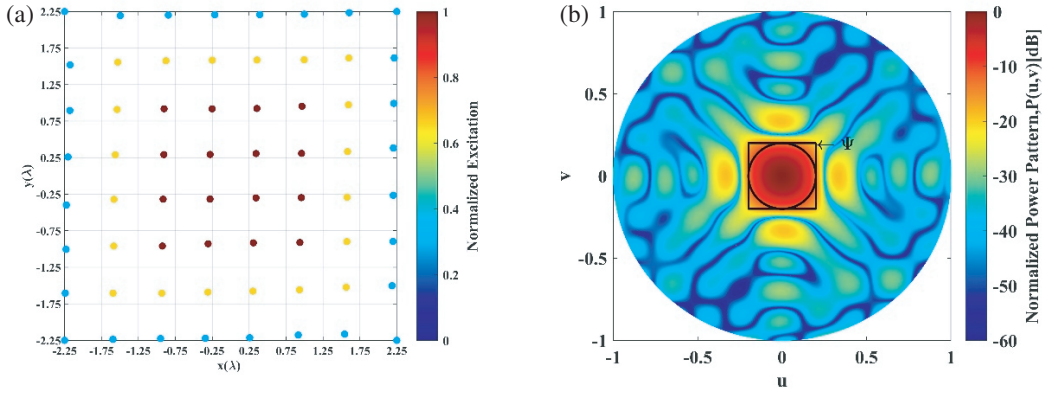

FIGURE 5. The simulation results of the LSNSPA when $N = 3$.

4. SIMULATION TESTING AND RESULTS ANALYSIS

In this part, we will use simulations to look into the MP-DWPSO-RS algorithm's optimization level and how well it works on different array models. We will also compare the MP-DWPSO-RS's optimization results to those of other algorithms to see how well it works. First, we utilize the MP-DWPSO-RS algorithm to optimize the LSNSPA array model. Next, to test the universality of the algorithm, we also apply it to a Symmetric Quadrant Sparse Rectangular Planar Array (SQSRPA) and Non-Uniformly Excited Sparse Rectangular Planar Array (NESRPA). Furthermore, we compare the optimization results of these three arrays with those from the literature, including the number of elements, the number of subarrays, sparsity ratio, BCE, and CSL. Finally, to illustrate the benefits of the MP-DWPSO-RS algorithm for the thorough optimization of the LSNSPA model, we conduct a comprehensive evaluation of the MP-DWPSO-RS algorithm against three other particle swarm optimization algorithms under the same constraints. The paper focuses solely on the research of beam patterns in a fixed vertical direction and does not address the issue of beam steering.

The parameters related to MP-DWPSO-RS are as follows: population particle number $NP = 50$, wavelength λ set to 1, learning factors $c_1 = c_2 = 2$, maximum iteration number $T = 200$, array aperture set to $L_x \times L_y = 4.5\lambda \times 4.5\lambda$, number of elements set to $M = 8 \times 8$, and receiving area $u_0 = v_0 = 0.2$.

All simulation experiments in this paper were conducted using an Intel Core i7-1250U CPU with a main frequency of 2.0 GHz, with a memory size of 16 GB, and the simulation software used was MATLAB R2021a.

4.1. Results of Array Optimization Using the MP-DWPSO-RS Algorithm

The first array model to be simulated is the LSNSPA array, which employs a large spacing distribution strategy, with its minimum element spacing $d_{\min}$ set to 0.6. Table 2 presents the comprehensive results after optimization using the MP-DWPSO-RS algorithm.

For subarray numbers 2, 3, and 4, the element positions and normalized power directions are shown in Figs. 4, 5, and 6, respectively.

TABLE 2. Results of the LSNSPA Optimization Using the MP-DWPSO-RS Algorithm.

N	$u_0 = v_0$	I_{sub}	$BCE/\%$	CSL/dB
2	0.2	0.8434, 0.3806	87.23	-15.78
3	0.2	0.8827, 0.5800, 0.2511	93.21	-13.79
4	0.2	0.9877, 0.7977, 0.5360, 0.2343	93.60	-13.53

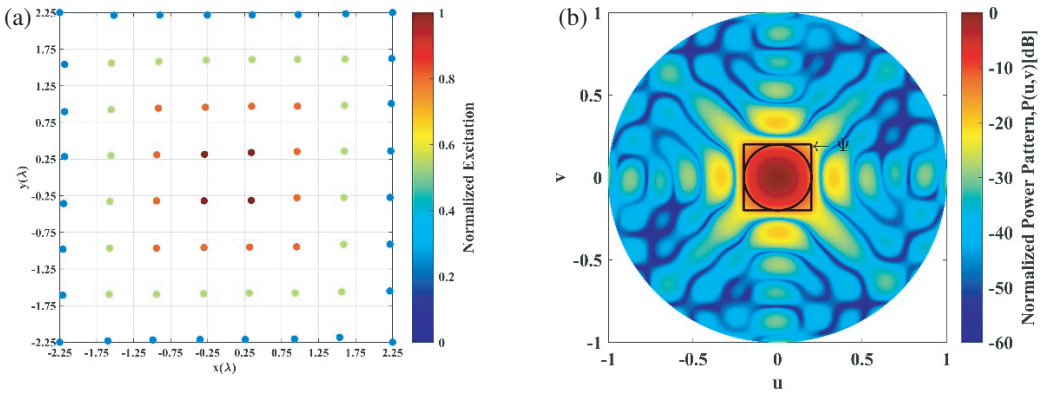

FIGURE 6. The simulation results of the LSNSPA when $N = 4$.

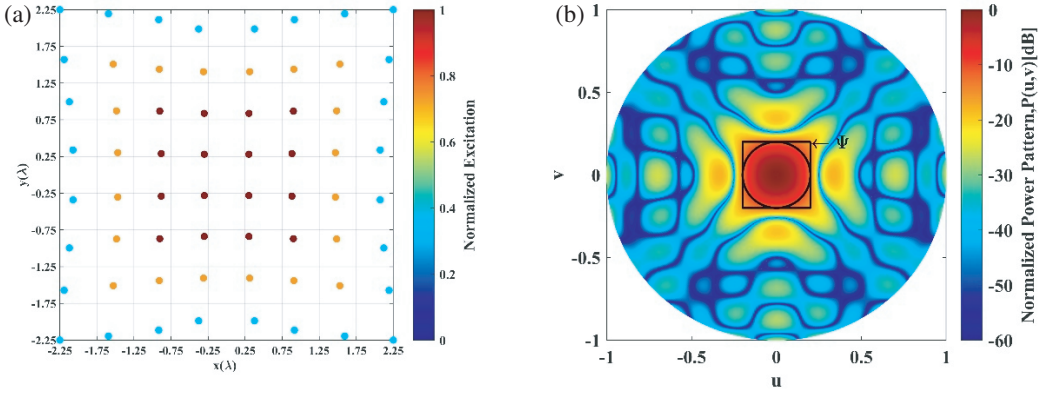

FIGURE 7. The simulation results of the SQSRPA when $N = 3$.

The second simulation model utilizes the SQSRPA array model with an aperture of $4.5\lambda \times 4.5\lambda$, consisting of 64 elements and a minimum element spacing of $d_{\min} = 0.5\lambda$. The results after comprehensive optimization using the MP-DWPSO-RS algorithm are presented in Table 3.

TABLE 3. Results of the SQSRPA Optimization Using the MP-DWPSO-RS Algorithm.

N	$u_0 = v_0$	I_{sub}	$BCE/\%$	CSL/dB
2	0.2	0.8304, 0.3887	90.15	-13.44
3	0.2	0.8555, 0.6223, 0.3001	91.38	-12.87
4	0.2	0.9737, 0.8043, 0.4323, 0.2941	91.78	-11.91

When the number of subarrays is 3, the element distribution and normalized power directions are shown in Fig. 7.

The final simulation model is the NESRPA model, which maintains consistent array parameters with the SQSRPA model. The results of comprehensive optimization using the MP-DWPSO-RS algorithm are presented in Table 4.

When the number of subarrays is 3, the element distribution and normalized power directions are shown in Fig. 8.

Through the simulation of the above three array types, we can understand that the BCE of all three arrays can reach over 90% when dividing just a few of subarrays. Among them, when the number of subarrays $N = 3$, the BCE of LSNSPA reaches over 93%, which is a relatively good optimization result for dividing only three subarrays, thus verifying the effectiveness of the MP-DWPSO-RS algorithm. Looking at the optimization results of the LSNSPA and NESRPA array models side by side, it is clear that, under the same conditions, arrays with a lot of space between them can improve their overall performance to achieve a high BCE and a low CSL.

TABLE 4. Results of the NESRPA Optimization Using the MP-DWPSO-RS Algorithm.

N	$u_0 = v_0$	I_{sub}	$BCE/\%$	CSL/dB
2	0.2	0.7753, 0.3185	88.23	-12.57
3	0.2	0.8531, 0.6563, 0.2797	91.51	-12.75
4	0.2	0.8741, 0.6736, 0.3461, 0.1219	91.81	-11.19

4.2. Comparison of MP-DWPSO-RS Algorithm with Other PSO Algorithms

To validate the superiority of the MP-DWPSO-RS algorithm in optimizing sparse planar arrays, this paper compares it with Basic PSO (Base-PSO) [10], Constricted Factor PSO (C-PSO) [11], and Dynamic Weighted PSO (DW-PSO) [12]. The tests were conducted on the NESRPA model with the following parameters set: population particle number $NP = 50$, wavelength λ set to 1, maximum iteration number $T = 200$, array aperture set to $L_x \times L_y = 4.5\lambda \times 4.5\lambda$, number of

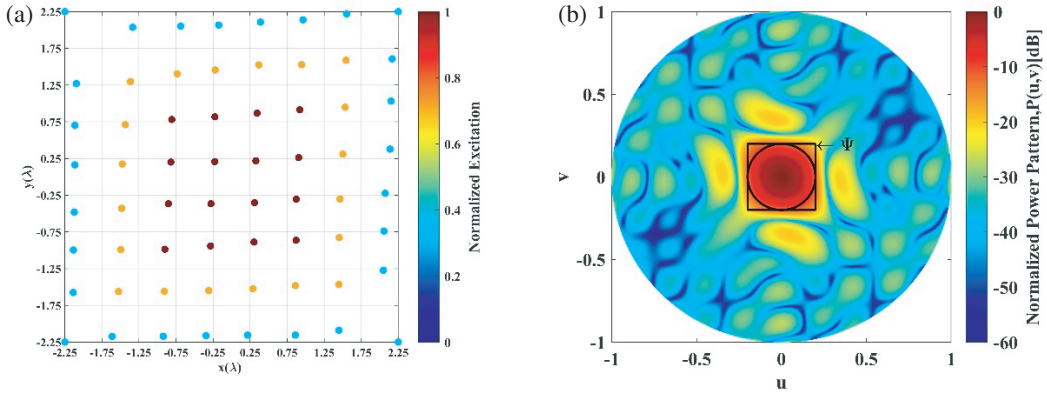

FIGURE 8. The simulation results of the NESRPA when $N = 3$.

TABLE 5. Comparison of comprehensive results of various arrays under rectangular receiving area.

	Ref. [9]	Ref. [13]	Ref. [14]	SQSRPA	NESRPA	LSNSPA
M	100	100	64	64	64	64
N	1	1	6	3	3	3
γ_e (%)	100	100	64	64	64	64
γ_a (%)	1	1	9.4	4.68	4.68	4.68
BCE (%)	86.48	91.09	91.11	91.38	91.51	93.21
CSL (dB)	-7.78	-14.68	-16.01	-12.87	-12.75	-13.79

elements set to $M = 8 \times 8$, number of subarrays $N = 3$, minimum element spacing $d_{\min} = 0.5\lambda$, receiving area set to $u_0 = v_0 = 0.2$, and the simulation software used in this paper is MATLAB R2021a.

Figure 9 shows that compared to other PSO algorithms, the MP-DWPSO-RS method produces superior simulation results. Relative to DW-PSO, the algorithm achieves higher BCE values in the early stages of iteration. This is mainly because the algorithm uses random side lengths of subarrays as optimization parameters, enabling the simultaneous optimization of element positions and subarray parameters during the iteration process, which significantly improves the overall efficiency of the optimization process and accelerates the search for the optimal value. Compared to C-PSO and Base-PSO, the algorithm adopts a nonlinear dynamic inertia weight, focusing on global search in the early stages of iteration and local search in the later stages, which helps to improve the convergence speed and search efficiency of the algorithm.

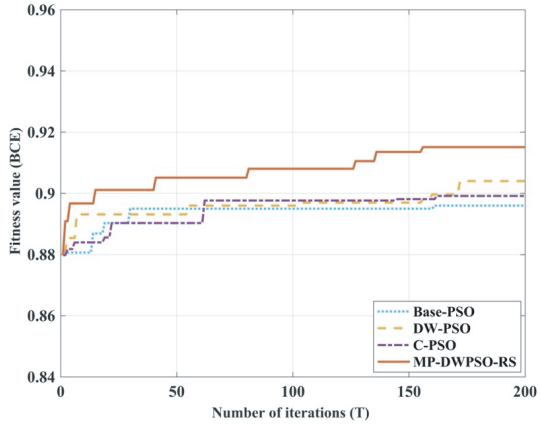

FIGURE 9. Simulation outcomes for various PSO algorithms.

4.3. LSNSPA Array Model Performance Comparison

For an emission array with the same aperture and reception area, the LSNSPA proposed in this paper employs a large-spacing distribution strategy and a subarray partitioning strategy, effectively reducing the number of array elements and amplifiers. By comparing it with the SQSRPA, NESRPA, and the array models optimized using the "one-step" method mentioned in [9, 13, 14], we will conduct a comparison in terms of the number of elements M, the number of subarrays N, element sparse distribution rate (γ_e), power amplifier sparse distribution rate (γ_a), BCE, and CSL.

Table 5 demonstrates that under the same conditions, the LSNSPA outperforms the SQSRPA and NESRPA, confirming the effectiveness of the large-spacing distribution strategy in enhancing array performance. By combining the large-spacing distribution strategy and subarray partitioning strategy, it is possible to achieve a high BCE value with a reduced number of subarrays, while taking into account both the expense and performance of the array.

5. CONCLUSION

In this paper, addressing the issue of achieving a high BCE value by dividing a few subarrays, an efficient subarray partitioning algorithm named MP-DWPSO-RS is proposed. This algorithm is a one-step approach that combines the large-spacing distribution strategy, subarray partitioning techniques, and dynamic weight particle swarm optimization, allowing for the simultaneous optimization of element positions, excitations, and subarray parameters. The algorithm takes the random side length of the subarrays as optimization parameters, achieving simultaneous optimization of positions and subarray partitioning side lengths during each iteration. This enhances the algorithm's global search capability while finding optimal values and avoiding local optima. Extensive simulations have shown that applying this algorithm to the LSNSPA can achieve a BCE of 93.21% by dividing only three

subarrays. Compared to other algorithms that require the division into three or more subarrays, when partitioning a few subarrays, this algorithm can significantly reduce the number of amplifiers and array elements, achieving a high BCE and low cost.

ACKNOWLEDGEMENT

This work was supported by the National Natural Science Foundation of China (Grant No. 51877151).

REFERENCES

[1] Lu, F., H. Zhang, W. Li, Z. Zhou, C. Zhu, C. Cheng, Z. Deng, X. Chen, and C. C. Mi, "A high-efficiency and long-distance power-relay system with equal power distribution," *IEEE Journal of Emerging and Selected Topics in Power Electronics*, Vol. 8, No. 2, 1419–1427, 2020.

[2] Kumar, S. and A. Sharma, "Switched beam array antenna optimized for microwave powering of 3-D distributed nodes in clustered wireless sensor network," *IEEE Transactions on Antennas and Propagation*, Vol. 70, No. 12, 11 734–11 742, 2022.

[3] Chen, X., "Power coverage analysis of cellular networks with energy harvesting and microwave power transfer-based power sharing," *IEEE Access*, Vol. 8, 77 204–77 213, 2020.

[4] Cao, W., J. Liu, J. Li, Q. Yang, and H. He, "Networked motion control for smart EV with multiple-package transmissions and time-varying network-induced delays," *IEEE Transactions on Industrial Electronics*, Vol. 69, No. 4, 4076–4086, 2022.

[5] Takabayashi, N., K. Kawai, M. Mase, N. Shinohara, and T. Mitani, "Large-scale sequentially-fed array antenna radiating flat-top beam for microwave power transmission to drones," *IEEE Journal of Microwaves*, Vol. 2, No. 2, 297–306, 2022.

[6] Jiang, H. and W. Dou, "Methods for improving the distance of microwave wireless power transmission with a given beam collection efficiency," *IEEE Antennas and Wireless Propagation Letters*, Vol. 19, No. 12, 2112–2116, 2020.

[7] Miao, K., Y. Zhang, C. Yao, and H. Sun, "Improved algorithm X for subarray partition with acceleration and sidelobe suppression," *IEEE Antennas and Wireless Propagation Letters*, Vol. 21, No. 7, 1403–1407, 2022.

[8] Liu, X., X. Zhang, and H. Yan, "Research of subarray partition in optically phased array radar," *Applied Science & Technology*, 2006.

[9] Oliveri, G., L. Poli, and A. Massa, "Maximum efficiency beam synthesis of radiating planar arrays for wireless power transmission," *IEEE Transactions on Antennas and Propagation*, Vol. 61, No. 5, 2490–2499, 2013.

[10] Poli, R., J. Kennedy, and T. Blackwell, "Particle swarm optimization: An overview," *Swarm Intelligence*, Vol. 1, 33–57, 2007.

[11] Cheng, Z., L. Fan, and Y. Zhang, "Multi-agent decision support system for missile defense based on improved PSO algorithm," *Journal of Systems Engineering and Electronics*, Vol. 28, No. 3, 514–525, 2017.

[12] Liu, Y., J. Xi, H. Bai, Z. Wang, and L. Sun, "A general robot inverse kinematics solution method based on improved PSO algorithm," *IEEE Access*, Vol. 9, 32 341–32 350, 2021.

[13] Li, J. and S. Chang, "Novel sparse planar array synthesis model for microwave power transmission systems with high efficiency and low cost," *Progress In Electromagnetics Research C*, Vol. 115, 245–259, 2021.

[14] Li, X., B. Duan, J. Zhou, L. Song, and Y. Zhang, "Planar array synthesis for optimal microwave power transmission with multiple constraints," *IEEE Antennas and Wireless Propagation Letters*, Vol. 16, 70–73, 2016.